




 Cite this: *RSC Adv.*, 2020, 10, 14235

# New diterpenoid quinones derived from *Salvia miltiorrhiza* and their cytotoxic and neuroprotective activities†

 Zhao-Kun Yin, Zi-Ming Feng, Jian-Shuang Jiang, Xu Zhang, Pei-Cheng Zhang \* and Ya-Nan Yang \*

One new tanshinone derivative, which possesses an unusual 6/6/5/6 fused-ring skeleton system (**1**), together with four new five-membered lactone benzohexa-membered ring compounds (**2**, **3**, **4A** and **4B**), and three new carboxyl substituted 5,5-spiroketal compounds (**5–7**), were isolated from the dried rhizomes of *Salvia miltiorrhiza*. The structures of these compounds were determined by multiple spectral analyses (UV, IR, NMR, and HR-ESI-MS). In addition, the absolute configurations were established by X-ray diffraction experiments, calculated and experimental circular dichroism spectra. Evaluation of antitumor activity showed that **1** had strong cytotoxicity to tumor-repopulating cells (TRCs) with an IC<sub>50</sub> value of 2.83 μM. In the evaluation of neuroprotective activity, **4A** and **6** showed a strong improvement in the survival rates of SK-N-SH cell injury induced by oxygen glucose deprivation (OGD).

 Received 3rd March 2020  
 Accepted 20th March 2020

DOI: 10.1039/d0ra02022b

[rsc.li/rsc-advances](http://rsc.li/rsc-advances)

## Introduction

Diterpenoid quinones are a kind of rosin diterpenes that are mainly composed of (11,12)-*o*-phenanthraquinone and (11,14)-*p*-phenanthraquinone. The root of *Salvia miltiorrhiza* Bunge (Labiatae) is known as a traditional Chinese medicine (TCM) which was found to be abundant in diterpenoid quinones.<sup>1–5</sup> Long-term pharmacological studies have found that diterpenoid quinones have significant activities, especially in terms of antitumor and cardiovascular activities.<sup>4–9</sup> In recent years, with continuous deep research on this kind of component from *S. miltiorrhiza*, new derivatizations of diterpenoid quinones have been discovered. For example, two diterpenoid quinones, which have a five-membered lactone benzohexa-membered ring structure,<sup>10</sup> and five 5,5-spiroketal,<sup>12–14</sup> have been isolated from *S. miltiorrhiza* Bunge (Labiatae), with these two components having neoteric basic skeleton forms of 6/6/5, 6/6/5/5 respectively. Although the amount of each compound was less, the discovery of these compounds with novel structures and significant activities reinvigorated our enthusiasm for the in-depth exploration of *S. miltiorrhiza*.

In a study of the biologically active constituents in the ethyl acetate-soluble portion of *S. miltiorrhiza* root bark, which was

acquired from an 80% EtOH extract, one new tanshinone derivative (**1**), which possessed an unusual ring-C compared with the common tanshinone skeleton, was obtained (Fig. 1). Furthermore, four new diterpenoid quinones (**2**, **3**, **4A** and **4B**), which all contained a 6/6/5 skeleton, and three new 5,5-spiroketal compounds (**5–7**) that had the feature of a carboxylic acid-substituted helical lactone ring, were isolated. Based on the source route analysis, these three types of components were all derived from (11,12)-*o*-phenanthraquinone or (11,14)-*p*-phenanthraquinone. Evaluation of antitumor activity and neuroprotective activity results of these isolated products were also reported.

## Results and discussion

Compound **1** was isolated as white amorphous powder. Its molecular formula was established as C<sub>18</sub>H<sub>16</sub>O<sub>5</sub> by its negative HRESIMS ion at *m/z* 311.0924 [M – H]<sup>–</sup> (calcd for C<sub>18</sub>H<sub>15</sub>O<sub>5</sub>, 311.0925), which indicated 11 degrees of unsaturation. The IR spectrum showed the absorptions of hydroxy (3433 cm<sup>–1</sup>), carbonyl (1725 cm<sup>–1</sup>) and olefinic (1616 cm<sup>–1</sup>) groups. Its <sup>1</sup>H NMR data (Table 1) were indicative of an AMX pattern for three aromatic protons at δ<sub>H</sub> 8.32 (1H, d, *J* = 8.5 Hz, H-1), 7.65 (1H, dd, *J* = 6.5, 8.5 Hz, H-2), and 7.61 (1H, d, *J* = 6.5 Hz, H-3) and a pair of *ortho*-aromatic protons at δ<sub>H</sub> 8.30 (1H, d, *J* = 8.5 Hz, H-6), 7.79 (1H, d, *J* = 8.5 Hz, H-7). This information, together with a methyl signal at δ<sub>H</sub> 2.72 (3H, s, H-18), indicated that **1** contained a 4-methylnaphthalene unit, which was similar to that of tanshinone I.<sup>19</sup> In addition, two oxygenated methylene protons at δ<sub>H</sub> 3.95 (1H, dd, *J* = 3.5, 12.0 Hz, H-15a), 3.15 (1H, t, *J* = 12.0 Hz, H-15b), one methine proton at δ<sub>H</sub> 2.28 (1H, m, H-16),

State Key Laboratory of Bioactive Substance and Function of Natural Medicines, Peking Union Medical College, Institute of Materia Medica, Chinese Academy of Medical Sciences, Beijing 100050, China. E-mail: pczhang@imm.ac.cn; yyn@imm.ac.cn; Fax: +86 10 63017757; Tel: +86 10 63165231

† Electronic supplementary information (ESI) available. CCDC 1975214. For ESI and crystallographic data in CIF or other electronic format see DOI: 10.1039/d0ra02022b



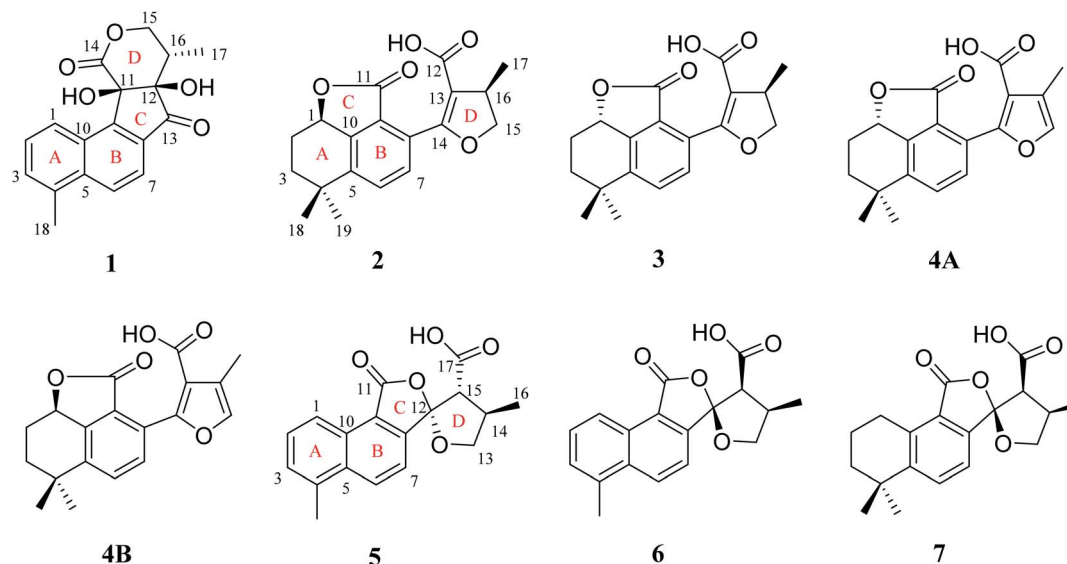


Fig. 1 The structures of compounds 1–7.

and one methyl signal at  $\delta_{\text{H}}$  0.93 (3H, d,  $J = 7.5$  Hz, H-17), were observed in the upfield region of the  $^1\text{H}$  NMR spectrum. The  $^{13}\text{C}$  NMR data (Table 1) and HSQC spectra revealed 18 carbon signals; apart from 11 carbons assigned to the 4-methylnaphthalene unit, the remaining seven carbons could be attributed to four quaternary carbons, one methine carbon, one methylene carbon and one methyl group. In the HMBC spectrum, the correlations from H-15 to C-12, C-16, and C-17, H-16 to C-12, C-

13, C-15, and C-17, as well as OH-12 to C-12, C-13, and C-16 revealed the presence of a 2,4-dihydroxy-3-methyl butanone moiety in 1 (Fig. 2). Additionally, the characteristic HMBC correlations from H-15 to C-14, H-7 to C-13, OH-11 to C-11, C-9, and C-12 established the unusual five-membered ring (ring C) and six-membered ring (ring D) in 1, which consisted of C-8/C-9/C-11/C-12/C-13 and C-11/C-12/C-14/O/C-15/C-16. Then, the

Table 1  $^1\text{H}$  NMR (500 MHz) and  $^{13}\text{C}$  NMR (125 MHz) data of compounds 1–4

No.	1 <sup>a</sup>		2 <sup>b</sup>		3 <sup>b</sup>		4A/4B <sup>b</sup>	
	$\delta_{\text{H}}$ ( $J$ in Hz)	$\delta_{\text{C}}$	$\delta_{\text{H}}$ ( $J$ in Hz)	$\delta_{\text{C}}$	$\delta_{\text{H}}$ ( $J$ in Hz)	$\delta_{\text{C}}$	$\delta_{\text{H}}$ ( $J$ in Hz)	$\delta_{\text{C}}$
1	8.32, d (8.5)	123.2	5.19, dd (5.5, 12.0)	78.0	5.19, dd (5.5, 12.0)	77.8	5.22, dd (5.5, 11.5)	77.8
2	7.65, dd (6.5, 8.5)	127.8	2.39, m, 1.62, m, 1.62, m	26.3	2.39, m, 1.62, m	26.3	2.40, m, 1.62, m	26.3
3	7.61, d (6.5)	130.5	1.92, m, 1.85, m	38.0	1.92, m, 1.85, m	38.2	1.92, m, 1.86, m	37.1
4		133.5		34.9		34.9		34.9
5		135.9		144.6		144.8		144.1
6	8.30, d (8.5)	128.4	7.55, d (8.0)	131.1	7.55, d (8.0)	131.5	7.65, d (8.0)	131.2
7	7.79, d (8.5)	118.3	7.47, d (8.0)	130.0	7.47, d (8.0)	130.0	7.52, d (8.0)	130.3
8		129.2		126.9		126.8		126.5
9		148.9		122.9		123.2		123.0
10		136.4		148.0		148.0		148.3
11		78.9		168.5		168.5		168.9
12		83.4		170.1		170.1		169.0
13		202.0		111.5		111.6		122.5
14		173.0		163.3		163.0		154.0
15	3.95, dd (3.5, 12.0), 3.15, t (12.0)	68.2	4.72, t, (9.0), 4.23, dd (5.5, 9.0)	78.9	4.70, t (9.0), 4.24, dd (5.5, 9.0)	78.9	7.32, s	140.6
16	2.28, m	40.5	3.49, m	37.2	3.40, m	37.1		117.0
17	0.93, d (7.5)	11.3	1.34, d (6.5)	19.6	1.38, d, (7.0)	20.0	2.23, s	10.1
18	2.72, s	19.6	1.44, s	31.8	1.44, s	31.8	1.45, s	31.8
19			1.19, s	30.9	1.19, s	31.0	1.22, s	31.0
OH-11	6.70, s							
OH-12	6.34, s							

<sup>a</sup> Data were measured in DMSO- $d_6$ . <sup>b</sup> Data were measured in  $\text{CDCl}_3$ .



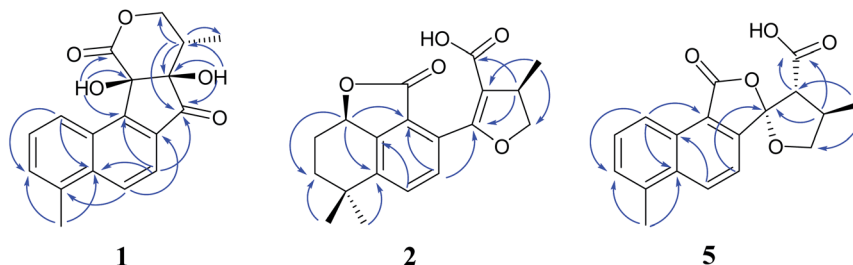


Fig. 2 Key HMBC correlations of compounds 1, 2, 5.

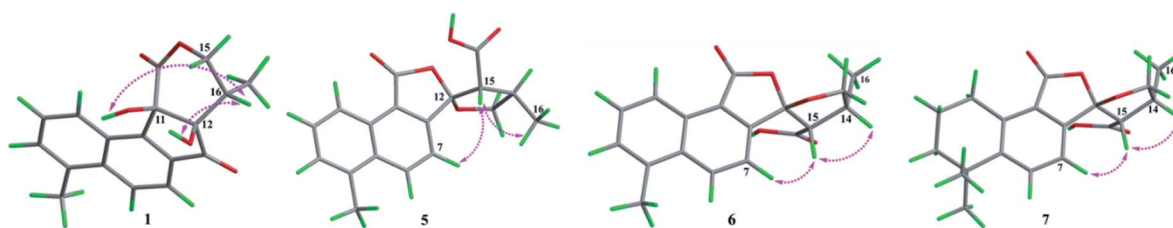


Fig. 3 The ROESY correlations of compounds 1, 5–7.

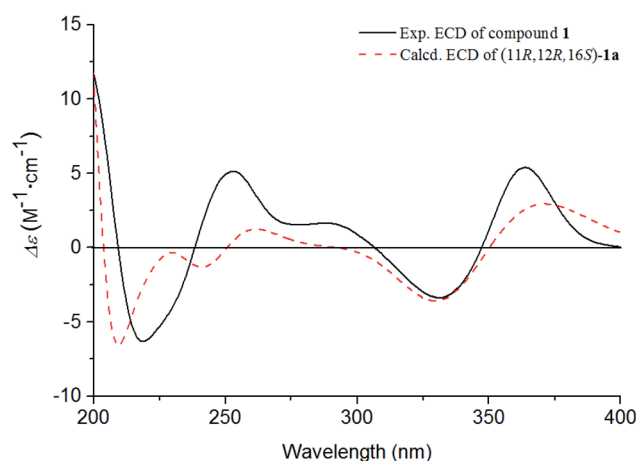
planar structure was elucidated as shown in Fig. 1 with a 6/6/5/6-membered ring skeleton.

The absolute configurations of C-11, C-12, and C-16 were identified by the ROESY experiment and comparison of the experimental and calculated ECD spectra. In the ROESY experiment, the correlations from OH-11 to H-16 and OH-12 confirmed the *cis*-relationship between OH-11 and H-16, as well as the *cis*-relationship between OH-11 and OH-12 (Fig. 3). This result was further verified by a strong correlation from OH-12 to H-16, together with a weak correlation from OH-12 to H-17. From the above analysis, **1** had only one pair of enantiomers (**1a**: 11*R*,12*R*,16*S* and **1b**: 11*S*,12*S*,16*R*). A systematic conformational analysis was performed for **1a** using a molecular mechanics force field (MMFF94) calculation. The optimized conformation of **1a** was further obtained using the time-dependent density functional theory (TDDFT) method at the B3LYP/6-311+G (d, p) level. The overall calculated ECD spectra of **1a** was established based on the Boltzmann weighting of the lowest energy conformers. Finally, the calculated ECD spectrum of **1a** was matched with the experimental result over the entire range of wavelengths (Fig. 4). Based on the above evidence, the structure of **1** was determined to be as shown in Fig. 1 and was named tanshin cyclopentanone A.

Compound **2**, obtained as white massive crystal, was indicated to have the molecular formula of C<sub>19</sub>H<sub>20</sub>O<sub>5</sub> according to the HRESIMS *m/z* 351.1198 [M + Na]<sup>+</sup> (calcd for C<sub>19</sub>H<sub>20</sub>NaO<sub>5</sub>, 351.1203). The IR spectrum indicated that **2** contained carboxyl (2955, 1766 cm<sup>-1</sup>) and carbonyl (1666 cm<sup>-1</sup>) functional groups. Its <sup>13</sup>C NMR data (Table 1) showed 19 carbon signals, including two carbonyl carbons, eight aromatic carbon signals and nine aliphatic carbon signals. In the <sup>1</sup>H NMR data (Table 1), a group of aromatic hydrogen signals appeared in the downfield region at δ<sub>H</sub> 7.55 (1H, d, *J* = 8.0 Hz, H-6), 7.47 (1H, d, *J* = 8.0 Hz, H-7). A set of -CH<sub>2</sub>CH<sub>2</sub>- characteristic signals were observed at δ<sub>H</sub> 2.39

(1H, m, H-2a), 1.62 (2H, m, H-2b), 1.92 (1H, m, H-3a), 1.85 (1H, m, H-3b). In the upfield region, based on the HSQC spectrum, the characteristic signals of a methyl substituted dihydrofuran ring at δ<sub>H</sub> 4.72 (1H, t, *J* = 9.0 Hz, H-15a), 4.23 (1H, dd, *J* = 5.5, 9.0 Hz, H-15b), 3.49 (1H, m, H-16), 1.34 (3H, d, *J* = 6.5 Hz, H-17) were observed. The 1D NMR information of **2** was almost identical to the 1*R*-hydroxy-anhydride of 16*R*-cryptotanshinone,<sup>15</sup> which was obtained *via* biotransformation by *Mucor rouxii*. Moreover, the HMBC correlations found in **2** were also the same as those of the 1*R*-hydroxy-anhydride of 16*R*-cryptotanshinone (Fig. 2).

However, the single-crystal X-ray diffraction experiment (Cu Kα radiation) showed that **2** possessed a 6/6/5 skeleton structure rather than a 6/6/7/5 skeleton of 1*R*-hydroxy-anhydride of 16*R*-cryptotanshinone (Fig. 5). This result showed that it is difficult to distinguish **2** and 1*R*-hydroxy-anhydride of 16*R*-cryptotanshinone

Fig. 4 Experimental and calculated ECD spectra of **1**.

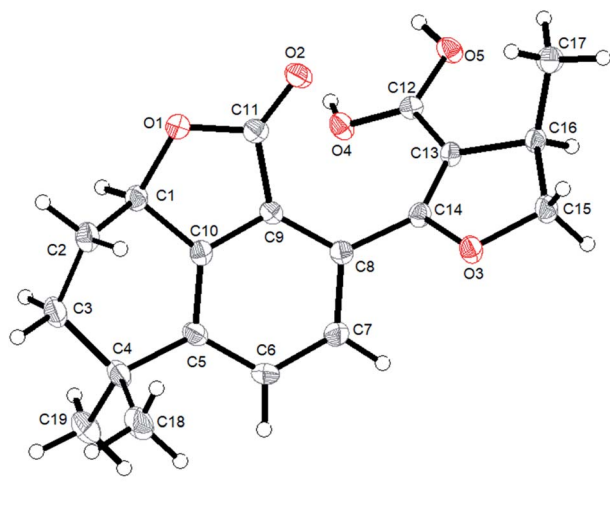


Fig. 5 ORTEP diagram of **2**.

only by using the 2D NMR data. The absolute configurations of **2** were determined to be *1R,16R* according to the X-ray diffraction analysis. This result was also confirmed by the calculated ECD data of (*1R,16R*)-**2**, which matched well with the experimental ECD data of **2** (Fig. S8, ESI<sup>†</sup>). Therefore, the structure of **2** was established and named salvianolactone acid A.

Compound **3** was isolated as white amorphous powder, and had the same molecular formula as **2** based on the HRESIMS  $m/z$  351.1198 [ $M + Na$ ]<sup>+</sup> (calcd for  $C_{19}H_{20}NaO_5$ , 351.1203). The UV spectrum and 1D, 2D NMR data of **3** were also similar to **2**, and these features illustrated that **3** possessed the same planar construction with **2**. However, the HPLC analysis and the nuances of the 1D NMR data between **2** and **3** indicated that **3**

not an enantiomer but an epimer of **2**. The absolute configurations of **3** might be **3a** (*1S,16R*) or **3b** (*1R,16S*). As a result of the experimental and calculated ECD spectra, the calculated ECD data of **3a** matched well with the experimental ECD data of **3** (Fig. S9, ESI<sup>†</sup>). Thus, the structure of **3** was determined and named salvianolactone acid B.

Compounds **4A** and **4B** are a pair of enantiomers, which were obtained through chiral *pre*-HPLC. Their molecular formulas was determined to be  $C_{19}H_{18}O_5$  based on the HRESIMS  $m/z$  325.1079 [ $M - H$ ]<sup>-</sup> (calcd for  $C_{19}H_{17}O_5$ , 325.1082). Analyzation of the 1D NMR data of **3** and **4A/4B** revealed that the main difference between **3** and **4A/4B** was ring D. The chemical shifts of C-15 ( $\delta_C$  140.6) and C-16 ( $\delta_C$  117.0) confirmed the furan ring moiety in **4A/4B**, which was supported by the HMBC correlations of CH<sub>3</sub>-17 with C-13, C-15, C-16, H-7 with C-5, C-9, C-14, and H-15 with C-13, C-14, C-16.

The absolute configurations of this pair of enantiomers were established by experimental and calculated ECD. As a result, the (*1S*)-enantiomer matched well with the experimental ECD spectra of **4A**, and the (*1R*)-enantiomer was in agreement with the experimental ECD spectra of **4B** (Fig. S10, ESI<sup>†</sup>). Therefore, the structures of **4A** and **4B** were elucidated and named salvianolactone acid C and salvianolactone acid D, respectively.

Compound **5**, a white amorphous powder, had the molecular formula of  $C_{18}H_{16}O_5$  as established by the HRESIMS ion at  $m/z$  311.0927 [ $M - H$ ]<sup>-</sup> (calcd for  $C_{18}H_{15}O_5$ , 311.0925). The IR spectrum indicated that **5** contained carbonyl groups (1762 and 1726  $cm^{-1}$ ). The <sup>1</sup>H NMR data (Table 2) of **5** was showed to have the typical structure of the methyl substituted naphthalene ring and included an AMX pattern at  $\delta_H$  8.78 (1H, d,  $J = 8.5$  Hz, H-1), 7.56 (1H, dd,  $J = 7.0, 8.5$  Hz, H-2), 7.44 (1H, d,  $J = 7.0$  Hz, H-3), a group of *ortho*-aryl hydrogen signals at  $\delta_H$  8.33 (1H, d,  $J = 8.5$  Hz, H-6), 7.55 (1H, d,  $J = 8.5$  Hz, H-7), and one methyl group

Table 2 <sup>1</sup>H NMR (500 MHz) and <sup>13</sup>C NMR (125 MHz) data of compounds 5–7 in CDCl<sub>3</sub>

No.	5		6		7	
	$\delta_H$ ( $J$ in Hz)	$\delta_C$	$\delta_H$ ( $J$ in Hz)	$\delta_C$	$\delta_H$ ( $J$ in Hz)	$\delta_C$
1	8.78, d (8.5)	122.5	8.82, d (8.5)	122.4	3.17, t (6.0)	26.1
2	7.56, dd (7.0, 8.5)	129.1	7.57, t (7.0, 8.5)	129.1	1.82, m	18.6
3	7.44, d (7.0)	128.7	7.45, d (7.0)	128.7	1.68, m	38.4
4		129.3		129.3		34.6
5		133.7		133.7		149.2
6	8.33, d (8.5)	132.3	8.32, d (8.5)	132.1	7.62, d (8.0)	133.2
7	7.55, d (8.5)	118.0	7.48, d (8.5)	117.7	7.18, d (8.0)	118.9
8		146.2		146.4		144.4
9		122.2		122.9		124.5
10		135.3		135.2		137.9
11		168.2		168.5		169.0
12		111.4		109.8		109.8
13	4.51, t (8.0), 3.85, t (8.0)	76.1	4.45, t (8.0), 4.07, dd (3.5, 8.5)	76.6	4.36 t (7.5), 3.97, dd (3.5, 8.5)	76.2
14	3.22, m	34.6	3.04, m	34.4	2.94, m	34.3
15	3.20, overlap	59.2	3.63, d (8.0)	54.7	3.48, d (8.0)	55.4
16	1.32, d (5.5)	17.1	1.43, d (7.0)	16.3	1.28, s	16.1
17		172.2		171.6		172.3
18	2.71, s	20.0	2.72, s	20.0	1.30, s	32.0
19					1.30, s	31.9



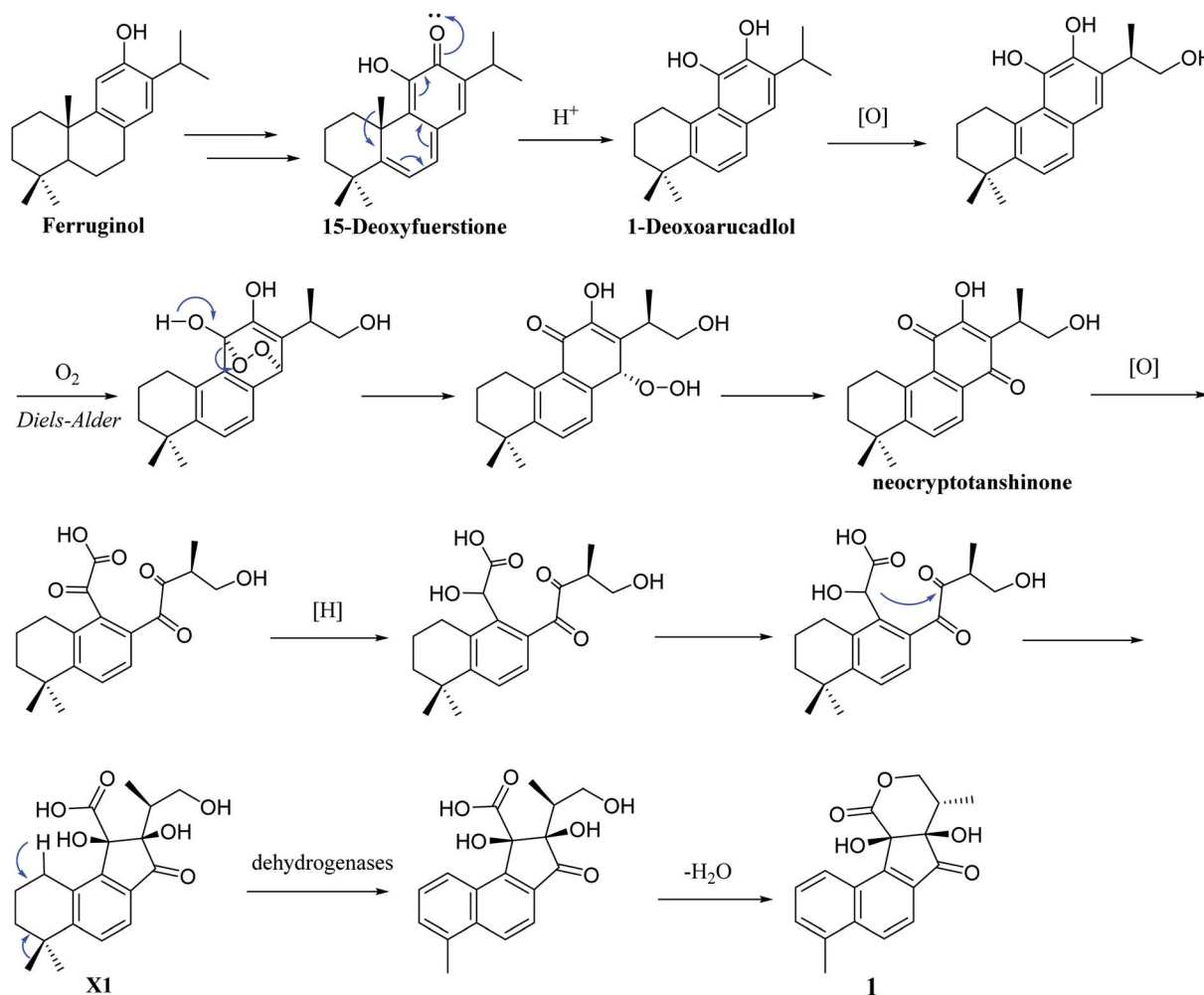
at  $\delta_{\text{H}}$  2.71 (3H, s, H-18). The  $^{13}\text{C}$  NMR data (Table 2) displayed 18 carbon signals; in addition to the 11 carbon signals on the methyl substituted naphthalene ring unit, **5** contained two carbonyl groups ( $\delta_{\text{C}}$  168.2, 172.2), one oxygenated quaternary carbon group ( $\delta_{\text{C}}$  111.4), two methine groups ( $\delta_{\text{C}}$  34.6, 59.2), one methylene group ( $\delta_{\text{C}}$  76.1) and one methyl group ( $\delta_{\text{C}}$  17.1). These NMR data were similar to those of *epi*-danshenspiroketallactone A,<sup>12</sup> except for the ethyl ester group in *epi*-danshenspiroketallactone A. The HMBC correlations (Fig. 2) of H-7 with C-5, C-9, C-12, CH<sub>3</sub>-16 with C-13, C-14, C-15, H-14 with C-17, and CH<sub>3</sub>-16 with C-17 were verified the planar structure of **5** as shown in Fig. 1.

In the case of CDCl<sub>3</sub> as a deuterated reagent, H-13 and H-16 overlapped. Therefore, DMSO-*d*<sub>6</sub> was used as the deuterated reagent, and these two signals can be separated and appeared at  $\delta_{\text{H}}$  3.59 (1H, d, *J* = 11.0 Hz, H-13) and 2.95 (1H, m, H-16), respectively (Table S1, ESI<sup>†</sup>). In the NOE spectrum (Fig. S56, ESI<sup>†</sup>), irradiation of CH<sub>3</sub>-16 enhanced H-15. Furthermore, the ROESY correlations (Fig. 3) of H-7 with H-15, H-15 with CH<sub>3</sub>-16 indicated that the absolute configurations of **5** might be **5a** (12*S*,14*R*,16*R*) or **5b** (12*R*,14*S*,16*S*). The calculated ECD spectra of **5a** and **5b** showed that **5a** agreed with the experimental

spectrum of **5** (Fig. S11, ESI<sup>†</sup>); therefore, the structure of **5** was determined and named *epi*-danshenspiroketallactone B.

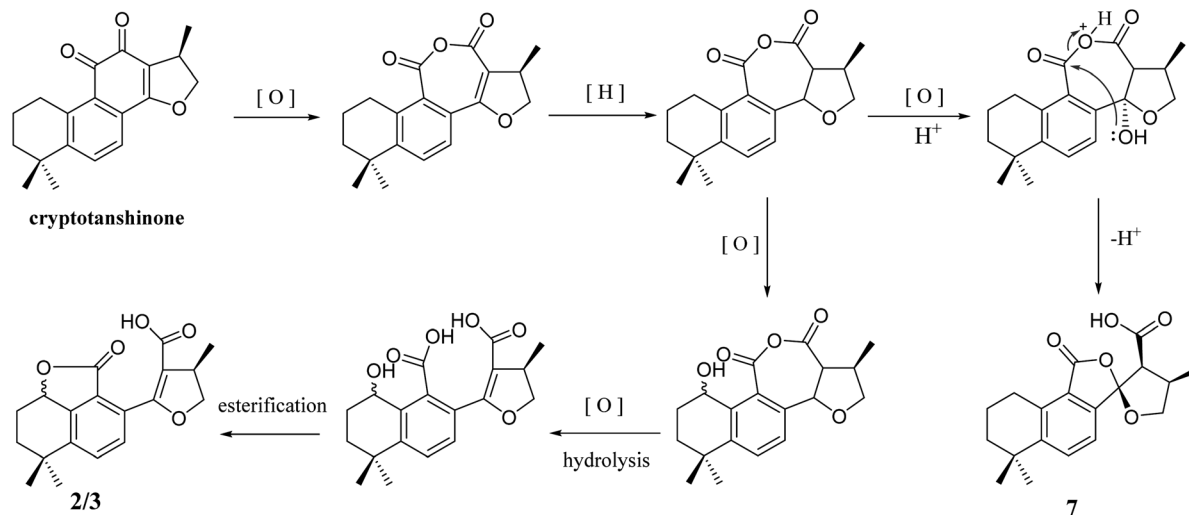
The planar structure of **6** was established as the same as **5** based on the 1D and 2D NMR data. The NOE spectrum (Fig. S67, ESI<sup>†</sup>) showed that irradiation with H-14 enhanced H-15. What's more, the ROESY experiment displayed that H-14 had correlation with H-15, and H-7 had correlation with H-15 (Fig. 3). Therefore, the absolute configurations of **6** might be **6a** (12*R*,14*R*,15*S*) or **6b** (12*S*,14*S*,15*R*). In the calculated ECD results, the spectrum of **6a** agreed with the experimental spectrum of **6** (Fig. S12, ESI<sup>†</sup>), so the structure of **6** was established and named *epi*-danshenspiroketallactone C.

Compound **7** was isolated as white amorphous powder and had the molecular formula of C<sub>19</sub>H<sub>22</sub>O<sub>5</sub> via the HRESIMS ion at *m/z* 329.1396 [M – H]<sup>–</sup> (calcd for C<sub>19</sub>H<sub>21</sub>O<sub>5</sub>, 329.1395). The  $^1\text{H}$  NMR data (Table 2) showed two aromatic protons, four methylene groups, two methine groups and three methyl groups. The  $^{13}\text{C}$  NMR spectrum (Table 2) of **7** displayed 19 carbon signals. Comparison of **7** with **6** showed that the main difference was in the structure of ring A. The chemical shifts of  $\delta_{\text{H}}$  3.17 (2H, t, *J* = 6.0 Hz, H-1), 1.82 (2H, m, H-2), 1.68 (2H, m, H-3) and  $\delta_{\text{H}}$  1.30 (6H, s, H-18,19) confirmed the dimethyl substituted six-



Scheme 1 Plausible biogenetic pathway for **1**.





Scheme 2 Plausible biogenetic pathway for 2/3 and 7.

membered ring of 7, which was also determined by the HMBC correlations of H-1 with C-2, C-3, C-5, C-9, C-10 and H-18/19 with C-3, C-4, and C-5.

In the NOE spectrum (Fig. S78, ESI<sup>†</sup>), irradiation of H-14 enhanced H-15. What's more, the ROESY correlations (Fig. 3) of H-15 with H-14, H-7 with H-15 illustrated that the absolute configurations of 7 might be either **7a** (12*R*,14*R*,16*S*) or **7b** (12*S*,14*S*,16*R*). Both **7a** and **7b** underwent ECD calculations, and **7a** matched the experimental spectrum of 7 (Fig. S13, ESI<sup>†</sup>), so the structure of 7 was finally determined and named *epi*-danshenspiroketallactone D.

Structurally, **1** represents a new skeleton of tanshinone derivative with an unusual 6/6/5/6-membered ring skeleton. Its distinctive biogenetic route is proposed in Scheme 1. A literature survey indicated that the essential precursor neocryptotanshinone,<sup>16</sup> which was isolated from the roots of *S. miltiorrhiza* previously, might be derived from ferruginol through a series of aromatization, oxidation, Diels–Alder reaction, rearrangement, hydrogenation and oxidation reactions. Subsequently, neocryptotanshinone formed **XI** through the oxidative cracking of ring C, hydrogenation, and cyclization. Finally, **1** was formed by aromatization and lactonization of **XI**. In particular, during the procedure of forming of **1**, the key process is the construction of a cyclopentanone moiety, which is unique in the tanshinone derivative. According to the above biosynthetic pathway perspective, the absolute configuration of C-16 remained constant during the progression of ring cracking and recycling of neocryptotanshinone.<sup>17,18</sup>

In addition, 2–7 contained two types of skeleton structures, which might all derive from cryptotanshinone (Scheme 2).<sup>11</sup> During a series of oxidation, hydrogenation, and cracking rearrangement of ring C/D under active enzymatic steps, cryptotanshinone could derive various products with multiple structures.<sup>10</sup>

TRCs play an important role during the process of tumor migration and recurrence. Therefore, it is a research hotspot to explore an effective targeted agent to kill TRCs. An *in vitro* assay

showed that **1** had strong cytotoxicity toward A375 TRCs (IC<sub>50</sub> = 2.83 μM), which were generated from a 3D fibrin gel culture system.<sup>20</sup> Delightedly, **1** exhibited no cytotoxicity to the nonstem-like A375 cancer cells at a concentration of 100 μM by the MTT method. This result implied that **1** might be a potent targeted antitumor agent with less adverse effects. In the evaluation of neuroprotective activities, **4A** showed obvious activity to increase the survival rate (13.08%) of SK-N-SH cell injury induced by oxygen glucose deprivation (OGD) compared with the positive control drug PHPB (7.43%). And under the same activity screening model, compound **6** also showed a noteworthy improvement in the survival rate (10.48%) compared with PHPB.

## Experimental

### General experimental procedures

The optical rotations and ECD spectra were experimented by RUDOLPH automatic V polarimeter JASCO V650 and J-815 spectrometer (JASCO, Easton, MD, USA), respectively. The UV spectra was measured on JASCO V-650. The IR data were measured on Nicolet 5700 spectrometer (Thermo Scientific, FL, USA). The NMR spectra were recorded with Bruker 500 MHz (Bruker-Biospin, Billerica, MA, USA) and 600 MHz NMR spectrometers (Varian, Inc., Palo Alto, CA, USA). HRESIMS reports were obtained from Agilent 6520 HPLC-Q-TOF (Agilent Technologies, Waldbronn, Germany). Preparative HPLC was performed using a Shimadzu LC-10AT with an ODS-A column (250 mm × 20 mm, 5 μm; YMC Corp., Kyoto, Japan). The Agilent 1260 series system coupled with an Apollo C18 column (250 mm × 4.6 mm, 5 μm; Alltech Corp., KY, USA) were used for HPLC-DAD experiments. RP-18 (50 μm, YMC Corp., Kyoto, Japan), Sephadex LH-20 (Pharmacia Fine Chemicals, Uppsala, Sweden), and silica gel (200–300 mesh, Qingdao Ocean Chemical Plant) were used as chromatographic substrates. Chiral-phase separation was performed by the Chiralpak AD-RH and AD-H chiral column (250 mm × 10 mm, 5 μm; Daicel Corp., Tokyo, Japan). Analytical chiral-phase HPLC was performed by



the Chiralpak AD-RH chiral column (250 mm × 4.6 mm, 5 μm; Daicel Corp., Tokyo, Japan).

### Fungal material

The dried rhizomes of *Salvia miltiorrhiza* were collected in Rizhao City (Shandong Province, China) in March 2017; the plant was authenticated by Lin Ma. A voucher specimen (herbarium no. ID-S-2944) has been deposited at the herbarium of the Department of Medicinal Plants, Institute of Materia Medica, Chinese Academy of Medical Sciences, Beijing, China.

### Extraction and isolation

The dried rhizomes of *Salvia miltiorrhiza* (70 kg) were smashed and extracted with 80% EtOH (3 × 100 L) at 85 °C for 2 h. The extract was concentrated under reduced pressure to obtained 23 kg of paste. Add water in the paste to make a suspension and extract four times with ethyl acetate. The ethyl acetate extract (2.2 kg) was subjected to silica gel (200–300 mesh) open column chromatography with a stepwise gradient of petroleum ether–acetone (100/0 to 0/100) gave twelve fractions (Fr.1–12). Fr.6 and Fr.7 (a total of about 100 g) were further subjected to column chromatography over silica gel and eluted with a gradient of PE–EtOAc to yield fractions y1–y30. Then, Fr.y22–Fr.y24 (27.6 g) was separated by silica gel column chromatography eluted with a gradient of PE–EtOAc mobile phase system and finally give six fractions A–F (2.38, 3.15, 5.87, 6.66, 6.89 and 1.80 g, respectively). Fraction E was further separated by Sephadex LH-20 (CH<sub>2</sub>Cl<sub>2</sub>–MeOH, gradient) and RP-HPLC (MeOH–H<sub>2</sub>O = 70 : 30 for first time; MeCN–H<sub>2</sub>O = 50 : 50 for second time) to yield compound 2 (82.6 mg), compound 3 (27.3 mg), compound 4A/4B (21.5 mg). Fr.y25–Fr.y29 (16.8 g) was separated by silica gel column chromatography eluted with a gradient of dichloromethane–methanol mobile phase system to yield five fractions A1–E1 (4.85, 3.16, 2.65, 3.22 and 2.53 g, respectively). Fraction D1 were further separated by Sephadex LH-20 (CH<sub>2</sub>Cl<sub>2</sub>–MeOH, gradient) and RP-HPLC (MeOH–H<sub>2</sub>O = 70 : 30 for first time; MeCN–H<sub>2</sub>O = 50 : 50 for second time) to yield compound 1 (4.9 mg), compound 5 (10.2 mg), compound 6 (21.0 mg), compound 7 (7.0 mg). The flow rate of the RP-HPLC was 1 mL min<sup>-1</sup>, and the detection wavelength was 254 nm.

**Tanshin cyclopentanone A (1).** White, amorphous powder;  $[\alpha]_{\text{D}}^{20} +173$  (*c* 0.1, MeOH); UV (MeOH)  $\lambda_{\text{max}}$  (log  $\epsilon$ ) 210 (2.10), 257 (2.51), 293 (1.69), 349 (1.22) nm; IR  $\nu_{\text{max}}$  3433, 2958, 2929, 1725, 1616, 1593, 1469, 1383, 1246, 1125, 1022, 822, 779 cm<sup>-1</sup>; CD (MeOH) 219 ( $\Delta\epsilon$  -6.30), 253 ( $\Delta\epsilon$  +5.13), 331 ( $\Delta\epsilon$  -3.37), 364 ( $\Delta\epsilon$  +5.38) nm; <sup>1</sup>H NMR (DMSO-*d*<sub>6</sub>, 500 MHz) and <sup>13</sup>C NMR (DMSO-*d*<sub>6</sub>, 125 MHz) spectroscopic data, see Table 1; HR-ESI-MS *m/z* 311.0924 [M - H]<sup>-</sup> (calcd for C<sub>18</sub>H<sub>15</sub>O<sub>5</sub>, 311.0925).

**Salvianolactone acid A (2).** White, massive crystal,  $[\alpha]_{\text{D}}^{20} -193.4$  (*c* 0.1, MeOH); UV (MeOH)  $\lambda_{\text{max}}$  (log  $\epsilon$ ) 210 (2.39), 241 (2.01), 308 (1.61) nm; IR  $\nu_{\text{max}}$  2955, 2649, 1766, 1666, 1493, 1338, 1247, 1072, 1007, 945, 844 cm<sup>-1</sup>; CD (MeOH) 215 ( $\Delta\epsilon$  +3.59), 234 ( $\Delta\epsilon$  -0.78), 260 ( $\Delta\epsilon$  +4.30), 322 ( $\Delta\epsilon$  -3.05); <sup>1</sup>H NMR (CDCl<sub>3</sub>, 500 MHz) and <sup>13</sup>C NMR (CDCl<sub>3</sub>, 125 MHz) spectroscopic data, see Table 1; HR-ESI-MS *m/z* 351.1198 [M + Na]<sup>+</sup> (calcd for C<sub>19</sub>H<sub>20</sub>NaO<sub>5</sub>, 351.1203).

**Salvianolactone acid B (3).** White, amorphous powder,  $[\alpha]_{\text{D}}^{20} +154$  (*c* 0.1, MeOH); UV (MeOH)  $\lambda_{\text{max}}$  (log  $\epsilon$ ) 210 (2.36), 240 (2.00), 304 (1.58) nm; IR  $\nu_{\text{max}}$  2961, 2871, 1767, 1664, 1497, 1440, 1072, 1045, 1005, 945, 843 cm<sup>-1</sup>; CD (MeOH) 231 ( $\Delta\epsilon$  +1.47), 257 ( $\Delta\epsilon$  -1.68), 296 ( $\Delta\epsilon$  +1.18) nm; <sup>1</sup>H NMR (CDCl<sub>3</sub>, 500 MHz) spectroscopic data and <sup>13</sup>C NMR (CDCl<sub>3</sub>, 125 MHz), see Table 1; HR-ESI-MS *m/z* 351.1198 [M + Na]<sup>+</sup> (calcd for C<sub>19</sub>H<sub>20</sub>NaO<sub>5</sub>, 351.1203).

**Salvianolactone acid C/D (4A/4B).** White, amorphous powder,  $[\alpha]_{\text{D}}^{20} +263$  (*c* 0.1, MeOH) (4A),  $[\alpha]_{\text{D}}^{20} -188$  (*c* 0.1, MeOH) (4B); UV (MeOH)  $\lambda_{\text{max}}$  (log  $\epsilon$ ) 207 (2.41), 241 (2.07), 295 (1.74), 329 (1.91) nm; IR  $\nu_{\text{max}}$  2961, 2868, 1766, 1687, 1554, 1490, 1435, 1301, 1219, 1069, 1005, 970, 841 cm<sup>-1</sup>; CD (MeOH) 240 ( $\Delta\epsilon$  +2.16), 262 ( $\Delta\epsilon$  -6.09), 325 ( $\Delta\epsilon$  +3.01) nm (4A), CD (MeOH) 239 ( $\Delta\epsilon$  -3.89), 261 ( $\Delta\epsilon$  +4.50), 325 ( $\Delta\epsilon$  -2.32) nm (4B); <sup>1</sup>H NMR (DMSO-*d*<sub>6</sub>, 500 MHz) spectroscopic data and <sup>13</sup>C NMR (CDCl<sub>3</sub>, 125 MHz), see Table 1; HR-ESI-MS *m/z* 325.1079 [M - H]<sup>-</sup> (calcd for C<sub>19</sub>H<sub>17</sub>O<sub>5</sub>, 325.1082).

**epi-Danshenspiroketallactone B (5).** White, amorphous powder,  $[\alpha]_{\text{D}}^{20} +39$  (*c* 0.1, MeOH); UV (MeOH)  $\lambda_{\text{max}}$  (log  $\epsilon$ ) 211 (2.44), 244 (2.39), 313 (1.65) nm; IR  $\nu_{\text{max}}$  3567, 2894, 1762, 1726, 1587, 1329, 1305, 1242, 1206, 1071, 985, 818 cm<sup>-1</sup>; CD (MeOH) 239 ( $\Delta\epsilon$  -7.52), 260 ( $\Delta\epsilon$  +4.13) nm; <sup>1</sup>H NMR (CDCl<sub>3</sub>, 500 MHz) and <sup>13</sup>C NMR (CDCl<sub>3</sub>, 125 MHz) spectroscopic data, see Table 2, <sup>1</sup>H NMR (DMSO-*d*<sub>6</sub>, 500 MHz) spectroscopic data, see Table S1 in ESI;† HR-ESI-MS *m/z* 311.0927 [M - H]<sup>-</sup> (calcd for C<sub>18</sub>H<sub>15</sub>O<sub>5</sub>, 311.0925).

**epi-Danshenspiroketallactone C (6).** White, amorphous powder,  $[\alpha]_{\text{D}}^{20} -38$  (*c* 0.1, MeOH); UV (MeOH)  $\lambda_{\text{max}}$  (log  $\epsilon$ ) 211 (2.37), 244 (2.33), 313 (1.59) nm; IR  $\nu_{\text{max}}$  3567, 3449, 2977, 1750, 1717, 1586, 1335, 1192, 1060, 974, 815 cm<sup>-1</sup>; CD (MeOH) 207 ( $\Delta\epsilon$  +1.90), 222 ( $\Delta\epsilon$  -0.94), 240 ( $\Delta\epsilon$  +3.86), 259 ( $\Delta\epsilon$  -2.75), 304 ( $\Delta\epsilon$  -0.93), 326 ( $\Delta\epsilon$  -0.76) nm; <sup>1</sup>H NMR (CDCl<sub>3</sub>, 500 MHz) and <sup>13</sup>C NMR (CDCl<sub>3</sub>, 125 MHz) spectroscopic data, see Table 2, <sup>1</sup>H NMR (DMSO-*d*<sub>6</sub>, 500 MHz) spectroscopic data, see Table S1 in ESI;† HR-ESI-MS *m/z* 311.0927 [M - H]<sup>-</sup> (calcd for C<sub>18</sub>H<sub>15</sub>O<sub>5</sub>, 311.0925).

**epi-Danshenspiroketallactone D (7).** White, amorphous powder,  $[\alpha]_{\text{D}}^{20} +4$  (*c* 0.1, MeOH); UV (MeOH)  $\lambda_{\text{max}}$  (log  $\epsilon$ ) 208 (2.44), 241 (1.63), 291 (1.18) nm; IR  $\nu_{\text{max}}$  3209, 2959, 1757, 1594, 1432, 1335, 1308, 1175, 1061, 927, 832 cm<sup>-1</sup>; CD (MeOH) 217 ( $\Delta\epsilon$  +1.50), 253 ( $\Delta\epsilon$  -1.25) nm; <sup>1</sup>H NMR (CDCl<sub>3</sub>, 500 MHz) and <sup>13</sup>C NMR (CDCl<sub>3</sub>, 125 MHz) spectroscopic data, see Table 2, <sup>1</sup>H NMR (DMSO-*d*<sub>6</sub>, 500 MHz) spectroscopic data, see Table S1 in ESI;† HR-ESI-MS *m/z* 329.1396 [M - H]<sup>-</sup> (calcd for C<sub>19</sub>H<sub>21</sub>O<sub>5</sub>, 329.1395).

### X-ray crystallographic data for salvianolactone acid A

Salvianolactone acid A (2) was recrystallized from CH<sub>2</sub>Cl<sub>2</sub> and MeOH (3 : 1) to give colorless block crystals. The X-ray crystallographic structure of 2 was obtained by anomalous scattering of Cu K $\alpha$  radiation. Crystal data: C<sub>19</sub>H<sub>20</sub>O<sub>5</sub>, *M* = 328.35, hexagonal, *a* = 14.63788(16) Å, *c* = 13.6616(2) Å, *U* = 2535.06(7) Å<sup>3</sup>, *T* = 109.90(10), space group *P*<sub>6</sub><sub>1</sub> (no. 172), *Z* = 6,  $\mu$ (Cu K $\alpha$ ) = 0.767, 14 929 reflections measured, 3057 unique (*R*<sub>int</sub> = 0.0262) which were used in all calculations. The final *wR*(*F*<sub>2</sub>) was 0.0771 (all data). Flack parameter, *x* = 0.09(6). The complete data were



deposited at the Cambridge Crystallographic Data Centre (CCDC 1975214).†

### Antitumor activities of compounds 1–7

The details evaluation method of antitumor activities is same as involved in the literature.<sup>20</sup>

### Neuroprotective activities of compounds 1–7

The screening method of neuroprotective activities refer to the literature.<sup>21</sup>

## Conclusion

A tanshinone derivative (**1**) with an unusual 6/6/5/6 skeleton structure, four new diterpenoid quinones (**2**, **3**, **4A** and **4B**), and three new 5,5-spiroketal compounds (**5**–**7**) were isolated from the roots of *Salvia miltiorrhiza*. All of the compounds were screened for their antitumor and neuroprotective activities. The results indicated that **1** had strong cytotoxicity to A375 TRCs (IC<sub>50</sub> = 2.83 μM); **4A** and **6** showed obvious neuroprotective activities based on the increased survival rate of SK-N-SH cell injury induced by oxygen glucose deprivation (OGD).

## Conflicts of interest

The authors have no conflicts of interest to declare.

## Acknowledgements

This research was financially supported by Fundamental Research Funds for CAMS/PUMC (2018RC350011), The Drug Innovation Major Project (2018ZX09711001-008), and the Chinese Academy of Medical Sciences (CAMS) Innovation Fund for Medical Sciences (No. 2017-I2M-3-010).

## References

- M. H. Li, Q. Q. Li, C. H. Zhang, N. Zhang, Z. H. Cui, L. Q. Huang and P. G. Xiao, *Acta Pharm. Sin. B*, 2013, **3**, 273–280.
- G. H. Du and J. T. Zhang, *Her. Med.*, 2004, **23**, 355–360.
- J. J. Wu, Q. L. Ming, X. Zhai, S. Q. Wang, B. Zhu, Q. L. Zhang, Y. B. Xu, S. S. Shi, S. C. Wang, Q. Y. Zhang, T. Han and L. P. Qin, *Carbohydr. Polym.*, 2019, **223**, 115125.
- C. Y. Su, Q. L. Ming, K. Rahman, T. Han and L. P. Qin, *Chin. J. Nat. Med.*, 2015, **13**, 163–182.
- Y. B. Wu, Z. Y. Ni, Q. W. Shi, M. Dong, H. Kiyota, Y. C. Gu and B. Cong, *Chem. Rev.*, 2012, **112**, 5967–6026.
- A. Watzke, S. J. O'Malley, R. G. Bergman and J. A. Ellman, *J. Nat. Prod.*, 2006, **69**, 1231–1233.
- D. J. Cousins, in *Medicinal, essential oil, culinary herb and pesticidal plants of the labiatae*, ed. D. J. Cousins, CAB International, Wallingford, Oxford, U.K., 1994, part 2, pp. 244–284.
- D. G. Kong, H. Oh, E. J. Sohn, T. Y. Hur, K. C. Lee, K. J. Kim, T. Y. Kim and H. S. Lee, *Life Sci.*, 2004, **75**, 1801–1816.
- B. Q. Wang, *J. Med. Plants Res.*, 2010, **4**, 2813–2820.
- L. Z. Li, X. Liang, X. Sun, X. L. Qi, J. Wang, Q. C. Zhao and S. J. Song, *Org. Biomol. Chem.*, 2016, **14**, 10050–10057.
- S. Y. Lee, C. D. Y. Choi and E. R. Woo, *Arch. Pharmacol. Res.*, 2005, **28**, 909–913.
- D. W. Zhang, X. Liu, D. Xie, R. D. Chen, X. Y. Tao, J. H. Zou and J. G. Dai, *Chem. Pharm. Bull.*, 2013, **61**, 576–580.
- H. W. Luo, S. X. Chen, J. N. Lee and J. K. Snyder, *Phytochemistry*, 1988, **27**, 290–292.
- F. Asari, T. Kusumi, G. Z. Zheng, Y. Z. Cen and H. Kakisawa, *Chem. Lett.*, 1990, **19**, 1885–1888.
- W. N. He, Y. Li, Y. J. Qin, X. M. Tong, Z. J. Song, Y. Z. R. Wei, L. Li, H. Q. Dai, W. Z. Wang, H. W. Luo, X. Ye, L. X. Zhang and X. T. Liu, *Appl. Microbiol. Biotechnol.*, 2017, **101**, 6365–6374.
- A. R. Lee, W. L. Wu, W. L. Chang, H. C. Lin and M. L. King, *J. Nat. Prod.*, 1987, **50**, 157–160.
- Y. Tomita and Y. Ikeshiro, *J. Chem. Soc., Chem. Commun.*, 1987, **520**, 1311–1313.
- N. Berova, K. Nakanishi and R. W. Woody, *Circular Dichroism: Principles and Applications*, Wiley, New York, 1994, pp. 413–442.
- M. J. Don, C. C. Shen, W. J. Syu, Y. H. Ding and C. M. Sun, *Phytochemistry*, 2006, **67**, 497–503.
- Y. Y. Liu, X. Y. Liang, X. N. Yin, J. D. Lv, K. Tang, J. W. Ma, T. T. Ji, H. F. Zhang, W. Q. Dong, X. Jin, D. G. Chen, Y. C. Li, S. Y. Zhang, H. D. Q. Xie, B. Zhao, T. Zhao, J. Z. Lu, Z. W. Hu, X. T. Cao, F. X. F. Qin and B. Huang, *Nat. Commun.*, 2017, **8**, 15207.
- S. W. Huang, J. W. Qiao, X. Sun, P. Y. Gao, L. Z. Li, Q. B. Liu, B. Sun, D. L. Wu and S. J. Song, *Funct. Foods*, 2016, **24**, 183–195.

